Electronic Supplementary Material (ESI) for Physical Chemistry Chemical Physics.


# +Supporting Information for the manuscript

# Metal-free recycling of waste polyethylene terephthalate mediated by TBD protic ionic salt: the crucial role of anionic ligand

*Chenxi Zhu[1], Linlin Yang[2], Chenhui Chen[1], Guixiang Zeng[2]*, Wei Jiang[1]**

1, State Key Laboratory of Pollution Control and Resources Reuse, School of the Environment, Nanjing University, Nanjing 210023, China

2, Kuang Yaming Honors School, Nanjing University, Nanjing 210023, China

*Corresponding author: jiangwei@nju.edu.cn

gxzeng@nju.edu.cn

## MATERIALS AND METHODS

**Materials.** PET plastics were collected from landfills and ground into particles with a 40–60 mesh size. 1,5,7-Triazabicyclo[4.4.0]dec-5-ene (TBD) was purchased from Shanghai Bide Pharmatech Technology Co. Ltd, China. nitric acid (HNO3), formic acid (HCOOH), propionic acid (PA), pyruvic acid (CH3COCOOH), and acetic acid (HOAc) were purchased from Nanjing Wanqing Chemical Glassware & Instrument Co., Ltd., China. EG and BHET standard samples were purchased from Shanghai Macklin Biochemical Technology Co., Ltd, China.

**Synthesis of TBD protic ionic salts.** First, a certain amount of TBD was dissolved in a flask with distilled water under the protection of nitrogen, and then, an equimolar amount of oxygenated organic acid (nitric acid, formic acid, propionic acid, pyruvic acid or acetic acid) was added into the TBD aqueous solution and magnetically stirred for 4 h. After this, the reaction product was evaporated with a rotary evaporator until crystals precipitated. Finally, the crystals were transferred to a vacuum oven for further drying at 70 ◦C for 12 h to obtain the target protic ionic salt, named HTBD-$NO_3$ HTBD-HCOO, HTBD-$CH_3CH_2COO$, HTBD-$CH_3COCOO$, and HTBD-OAc.

**General procedure for PET glycolysis.** For the catalytic experiments, a 25 mL three-necked flask equipped with a mechanical stirrer was filled with 1.0 g of PET (W1) and a certain amount of EG. The catalysts were added to the flask when the mixture was heated to the target temperature. Degradation reactions were carried out in a temperature range from 150 ◦C to 200 ◦C for 20–240 min under atmospheric pressure. When the reaction was completed, 300 mL of distilled water was added to the reaction

solution. Unreacted PET particles were separated by filtration. The collected material was dried at 80 ◦C for 4.0 h and weighed ($W_2$). The volume of the filtrate was adjusted to 1 L and the production of BHET was determined by high-performance liquid chromatography (HPLC). The conversion of PET and the yield of BHET were calculated by Eq. (1) and (2) as follows:

$$Conversion\ of\ PET = \frac{w_1 - w_2}{w_1} \times 100\%$$

$$Yield\ of\ BHET = \frac{n_{BHET}}{n_{initial-PET}} \times 100\%$$

where $w_1$ is the initial weight of PET and $w_2$ is the weight of unreacted PET. $n_{BHET}$ is the production of BHET; $n_{initial\text{-}PET}$ is the molecular weight of BHET by the original PET mole number.

**The reuse of protic ionic salt**. After the main product was separated, the light-yellow concentrated liquid was rotary evaporated again until no moisture remained, and then, the material was dried in a vacuum oven for 12 h to obtain a dispersion containing EG and the ionic salt, which was used as a solvent and a catalyst for the reusability experiment. Apart from replenishing EG, the recovered solvent and catalyst were directly utilized in the next cycle

**Characterization.** The morphologies of the initial PET and residual PET were evaluated by environmental scanning electron microscopy (ESEM, FEI Quanta 250 FEG, USA) at an accelerating voltage of 2.5 kV. Thermal analysis of the main product was performed with DSC at a heating rate of 10 ℃/min from 10 ℃ to 250 ℃ by using a DSC Q20 (TA Instruments, USA) under a nitrogen atmosphere. Thermal analysis of

the synthesized ionic slats was performed with TGA by heating the sample from 25 ℃ to 600 ℃ at a rate of 10 ℃/min. The contents of the degradation product were analyzed with HPLC, equipped with a refractive index detector and a BET C18 column, under an oven temperature of 30 ℃. The mobile phase was a mixture of 50% methanol and 50% water, and the flow rate was 0.1 mL min-1. The structures of the synthesized protic ionic salts were determined with an FT-IR spectrometer (Nicolet iS5, USA) by using KBr as the blank in the range of 4000–400 $cm^{-1}$ and an NMR apparatus (Bruker DRX500, Germany). The molecular weights of the initial PET and main product were determined by gel permeation chromatography (GPC, Agilent PL-GPC 50, USA).

**Computational details.** All calculations were performed by the density functional theory (DFT) method[1, 2] with the ωB97XD functional[3] in the solution phase (ethylene glycol, EG)[4]. The solvation effect was considered with the solvation model based on density (SMD)[5]. In the calculations, the 6-31++G** basis sets[6-9] were used for ethylene glycol and hydrogen (H) atoms connected to nitrogen (N) in HTBD-anion catalysts. For other atoms, the 6-31+G* basis sets[6-9] were utilized. Vibrational frequency calculations were performed for each structure to ensure whether it is a minimum (no imaginary frequency) or a transition state (TS, only one imaginary frequency) on the potential energy surfaces. To validate the connection between the reactant and product, the intrinsic reaction coordinate (IRC) [10, 11] calculations were conducted for each transition state. The Gibbs energy in solution was calculated at the experimental temperature (463.15 K), where the translational entropy was corrected with the method developed by Whitesides et al[12]. All of these calculations were carried out with the Gaussian 16

program[13]. The IGMH[14] (independent gradient model based on Hirshfeld partition) analysis was carried out using Multiwfn[15] 3.8 program package.

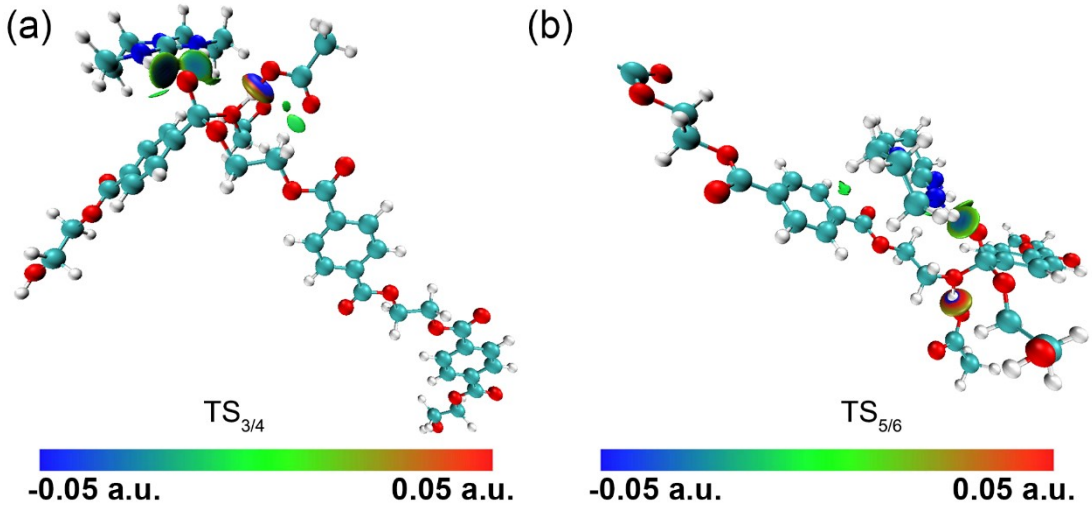


**Fig S1.** IGMH analysis of (a) $TS_{3/4}$ and (b) $TS_{5/6}$ for glycolysis of PET mediated by the HTBD-OAc ionic salt.

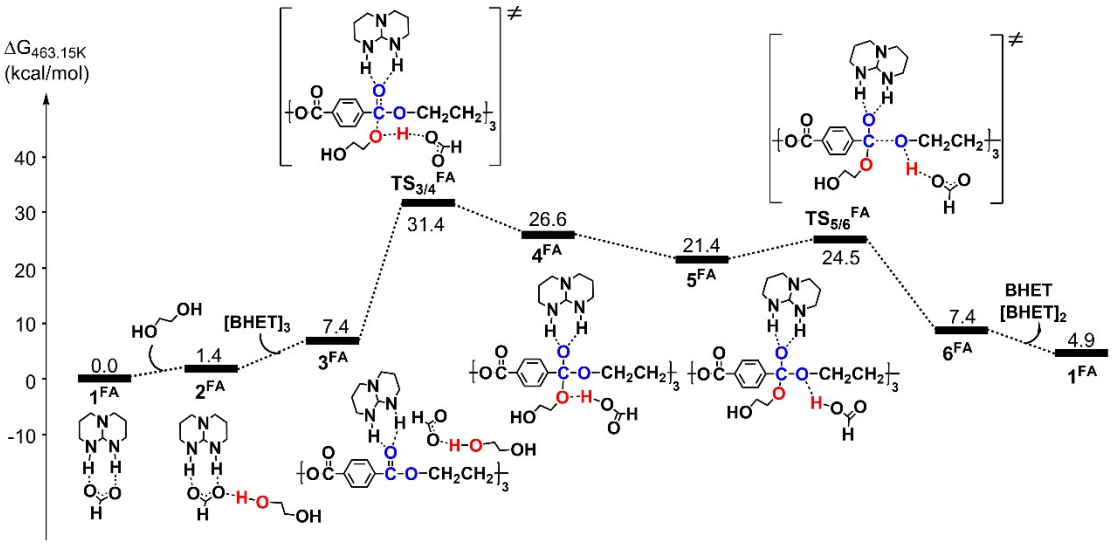


**Fig S2.** Gibbs free energy profiles for the glycolysis of PET by EG mediated by the HTBD-HCOO protic ionic salt.

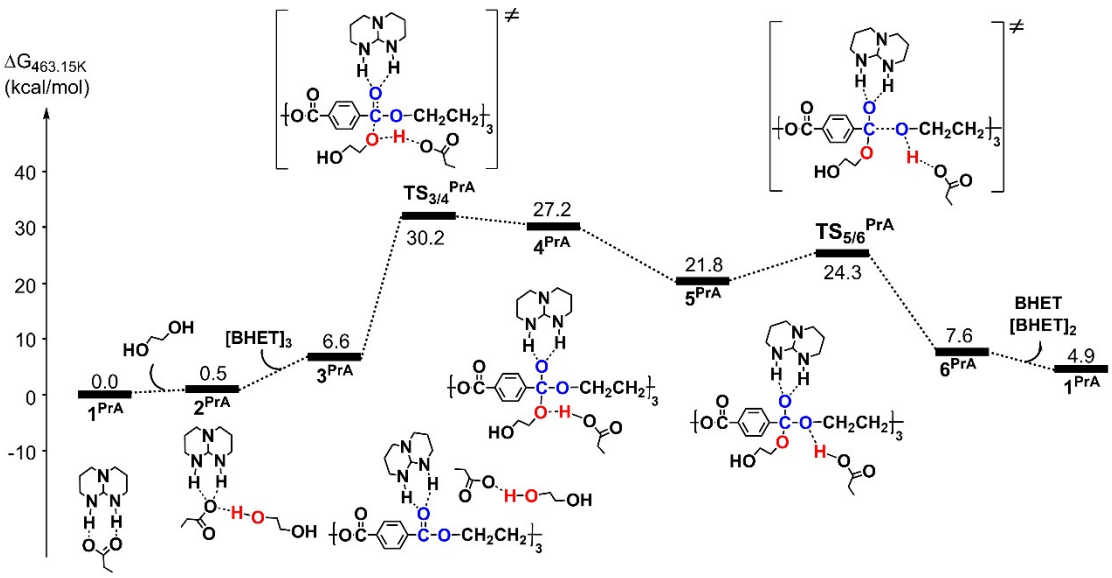


**Fig S3.** Gibbs free energy profiles for the glycolysis of PET by EG mediated by the HTBD-$CH_3CH_2COO$ protic ionic salt.

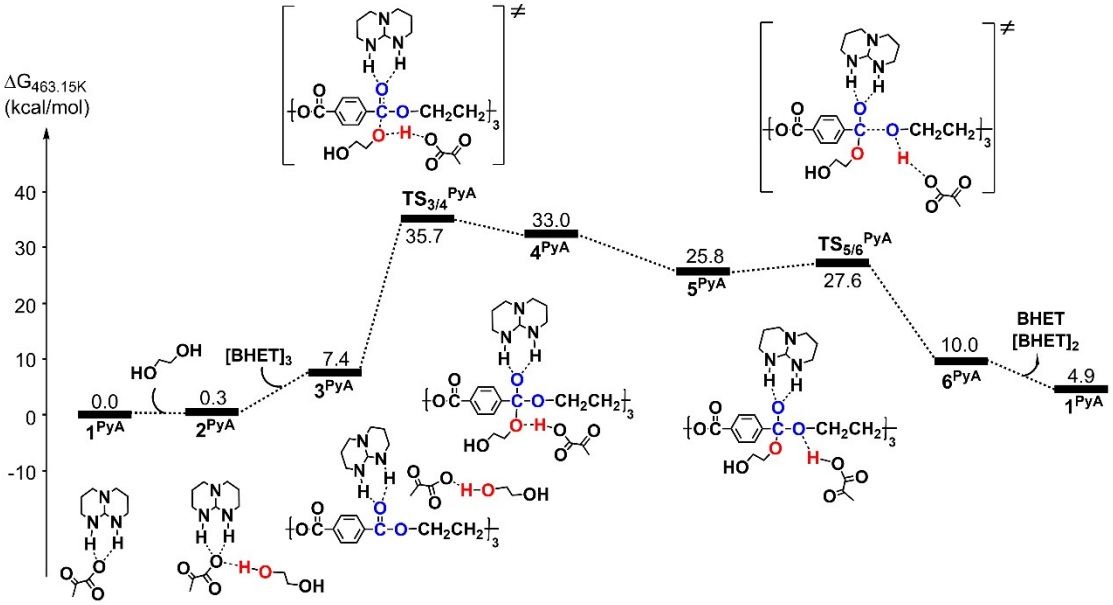


**Fig S4.** Gibbs free energy profiles for the glycolysis of PET by EG mediated by the HTBD-$CH_3COCOO$ protic ionic salt.

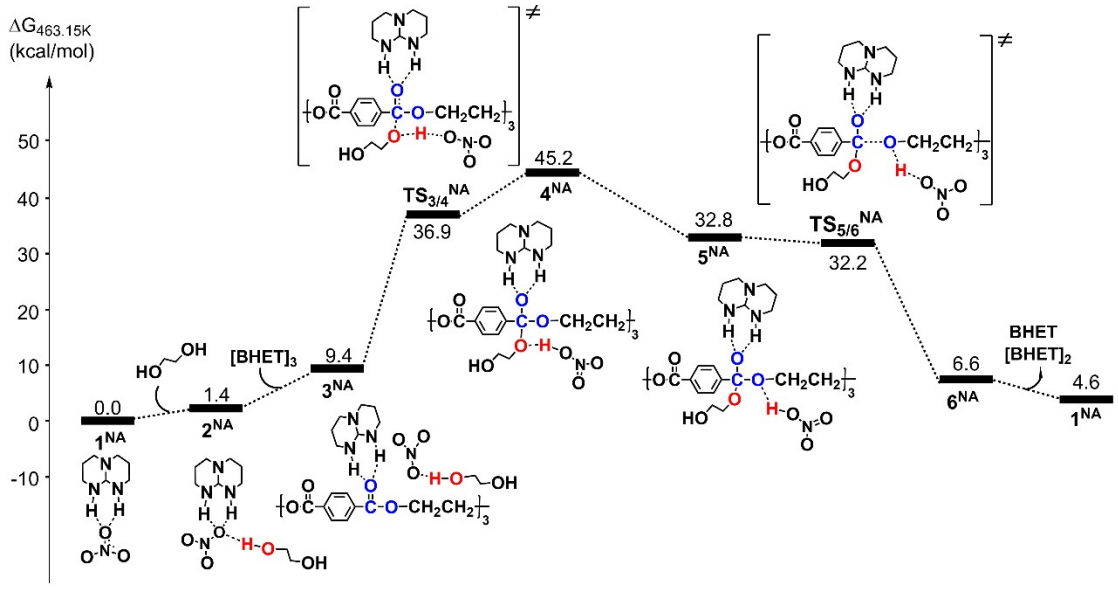


**Fig S5.** Gibbs free energy profiles for the glycolysis of PET by EG mediated by the HTBD-$NO_3$ protic ionic salt.

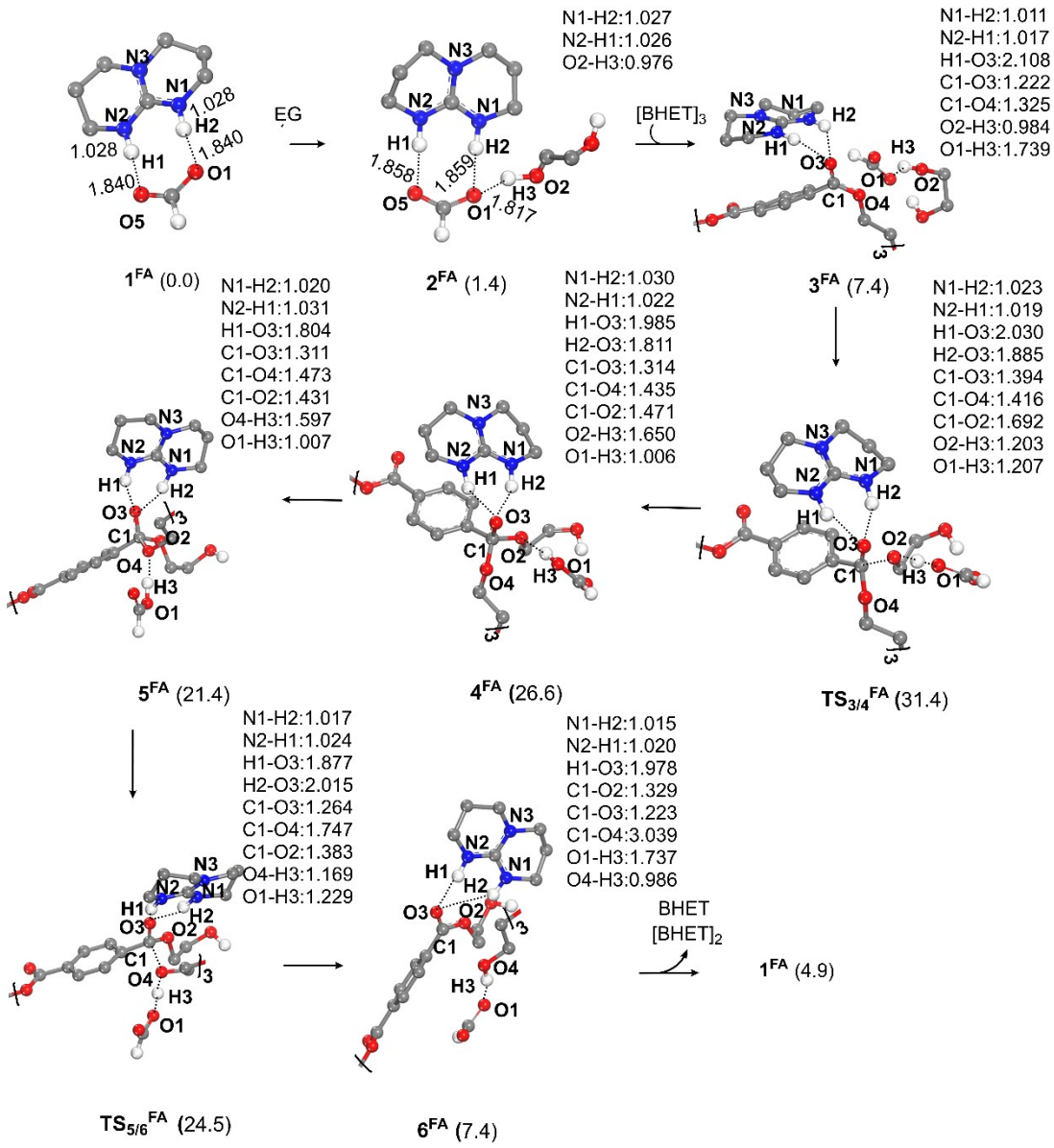


**Fig S6.** Optimized geometries of all species involved in the glycolysis of PET by EG mediated by the HTBD-HCOO protic ionic salt. Distances are in angstrom. The Gibbs energy changes are given in parentheses (kcal/mol).

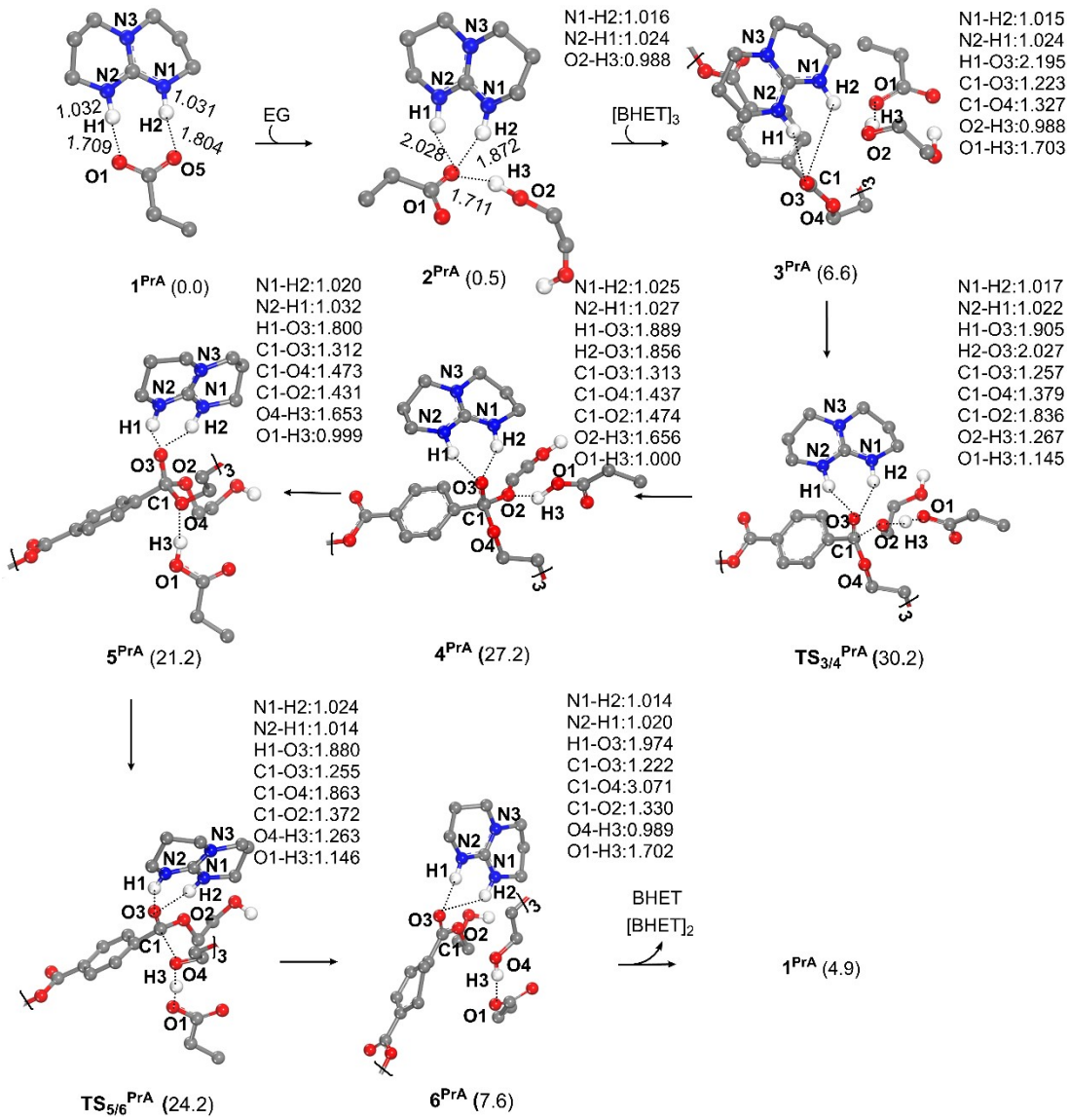


**Fig S7.** Optimized geometries of all species involved in the glycolysis of PET by EG mediated by the HTBD-$CH_3CH_2COO$ protic ionic salt. Distances are in angstrom. The Gibbs energy changes are given in parentheses (kcal/mol).

FA

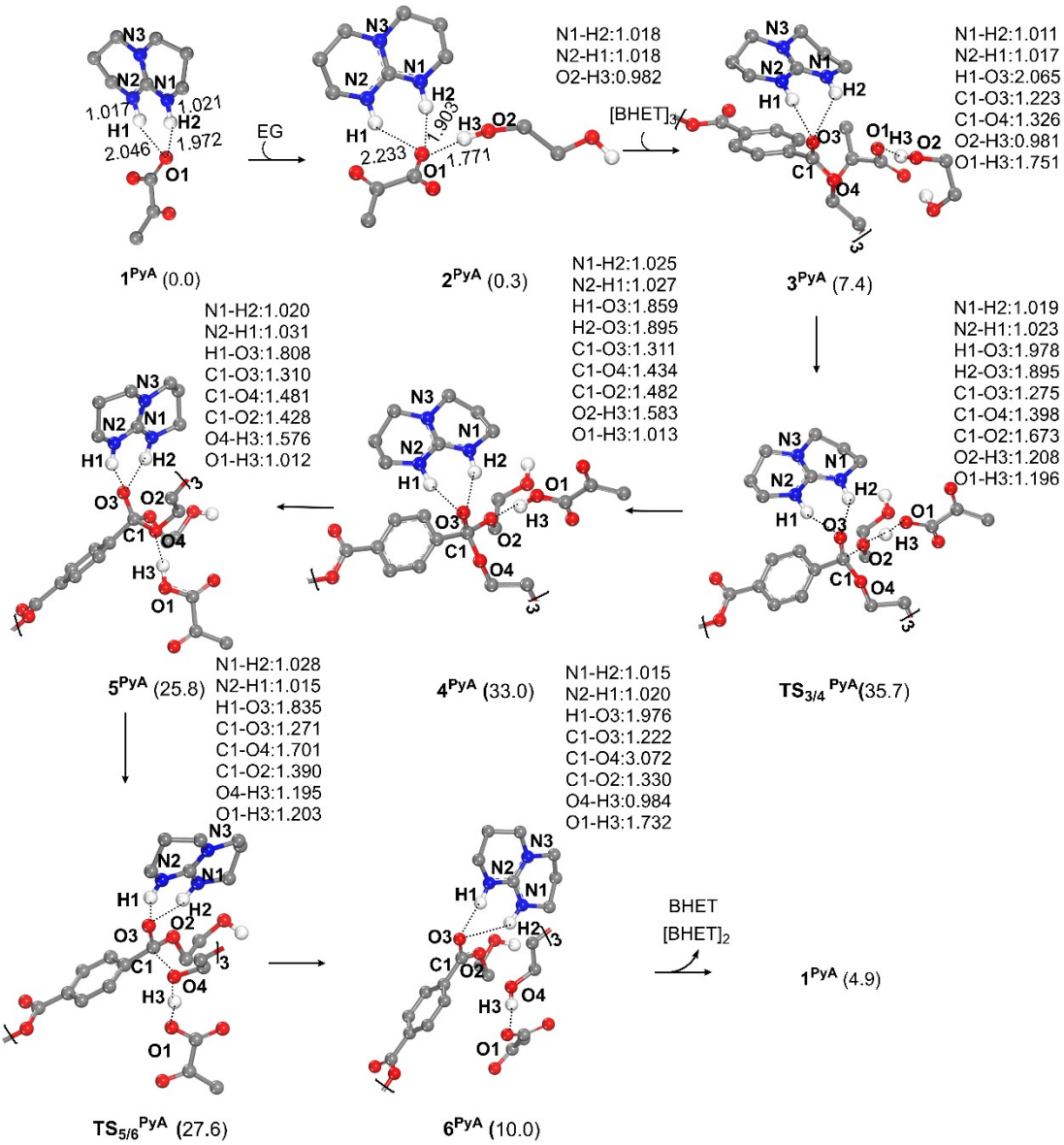


**Fig S8.** Optimized geometries of all species involved in the glycolysis of PET by EG mediated by the HTBD-$CH_3COCOO$ protic ionic salt. Distances are in angstrom. The Gibbs energy changes are given in parentheses (kcal/mol).

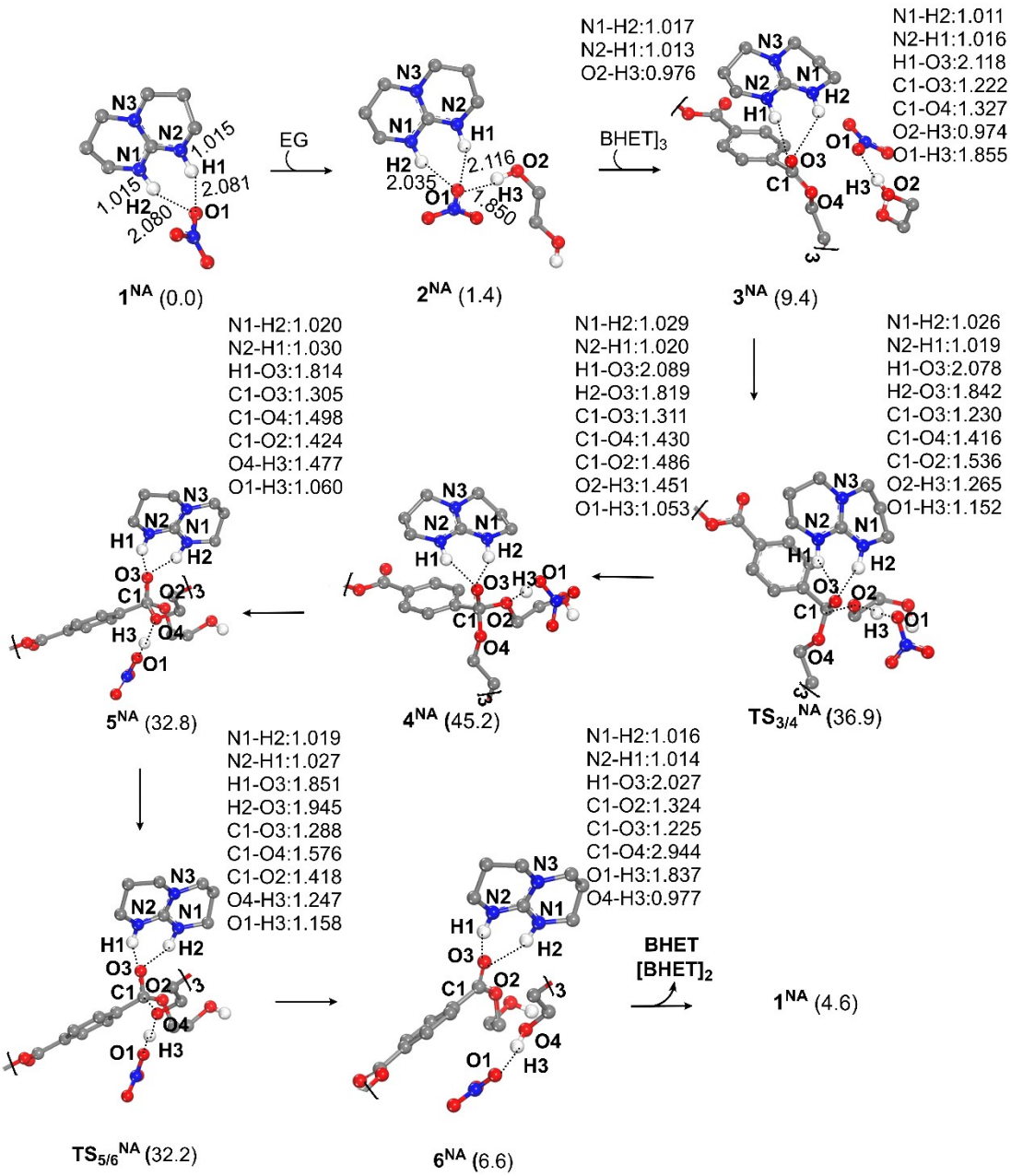


**Fig S9.** Optimized geometries of all species involved in the glycolysis of PET by EG mediated by the HTBD-$NO_3$ protic ionic salt. Distances are in angstrom. The Gibbs energy changes are given in parentheses (kcal/mol).

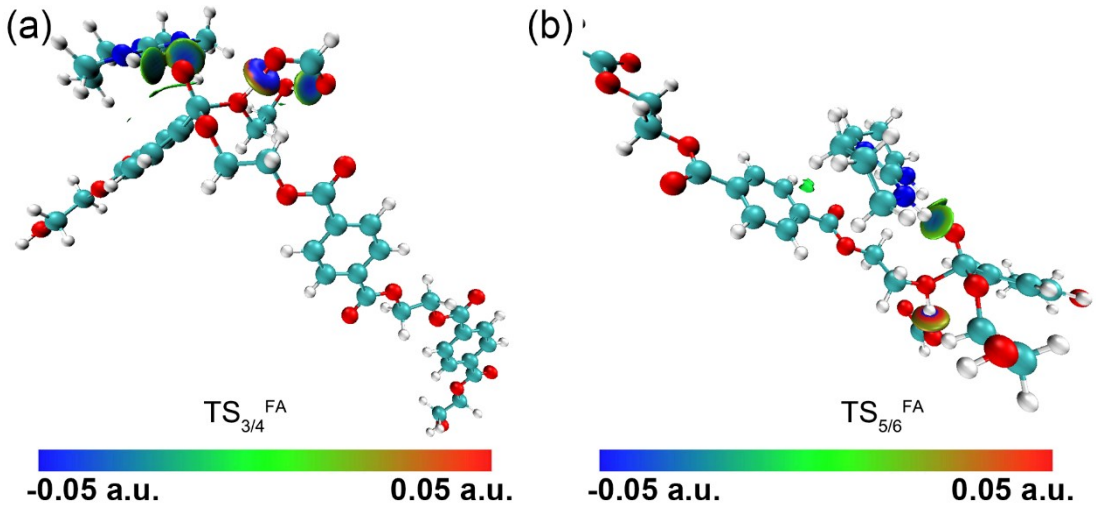


**Fig S10.** IGMH analysis of (a) $TS_{3/4}$ and (b) $TS_{5/6}$ for glycolysis of PET mediated by the HTBD-HCOO ionic salt.

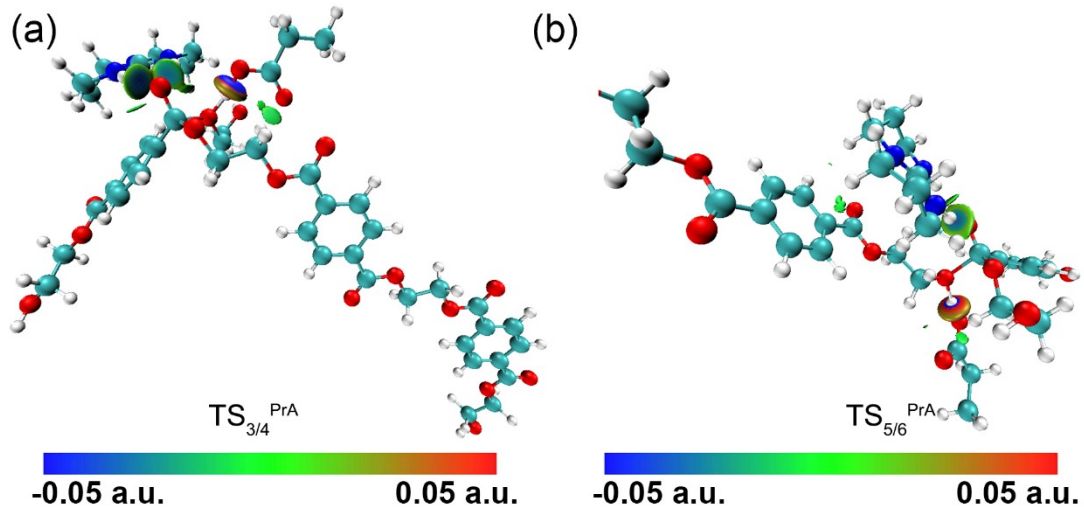


**Fig S11.** IGMH analysis of (a) $TS_{3/4}$ and (b) $TS_{5/6}$ for glycolysis of PET mediated by the HTBD-$CH_3CH_2COO$ ionic salt.

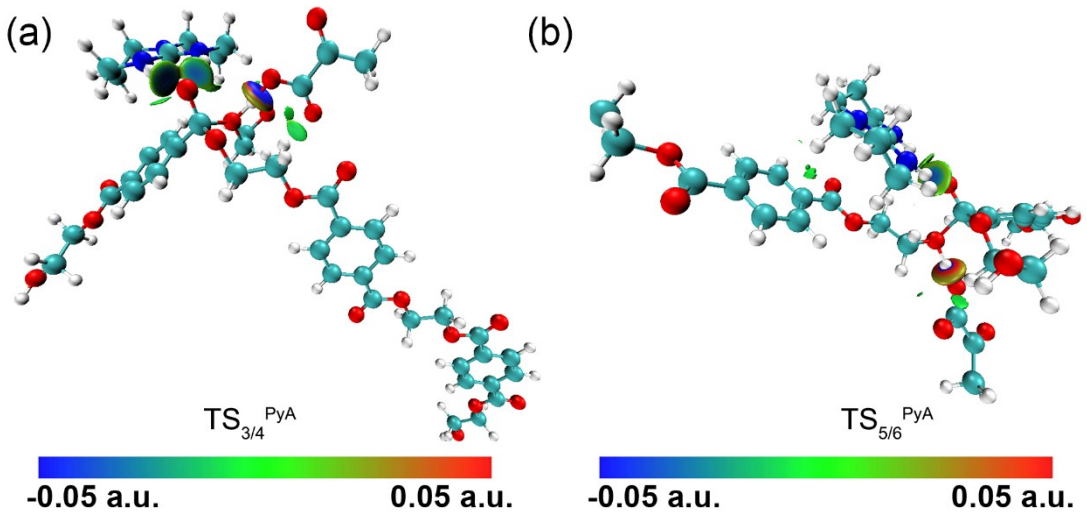


**Fig S12.** IGMH analysis of (a) $TS_{3/4}$ and (b) $TS_{5/6}$ for glycolysis of PET mediated by the HTBD-$CH_3COCOO$ ionic salt.

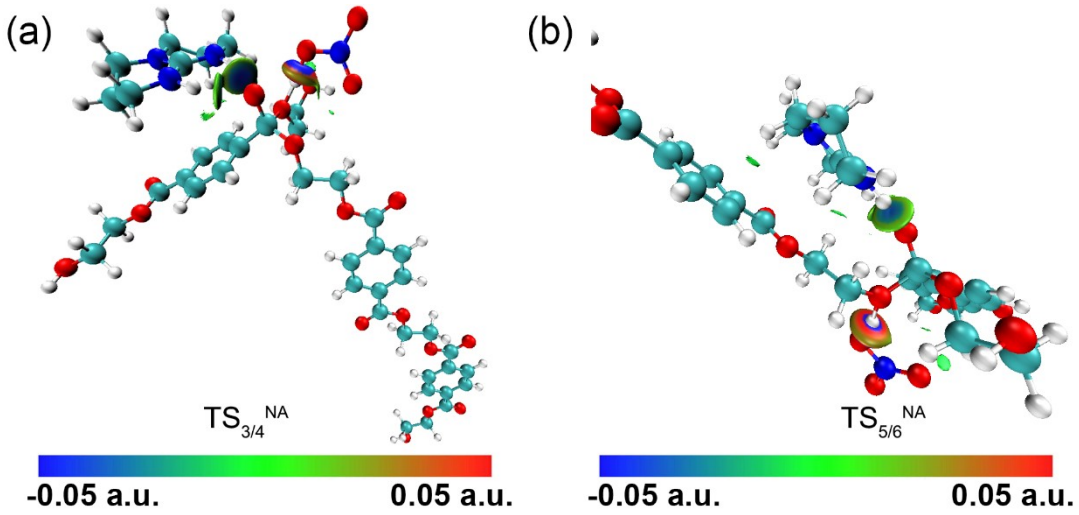


**Fig S13.** IGMH analysis of (a) $TS_{3/4}$ and (b) $TS_{5/6}$ for glycolysis of PET mediated by the HTBD-$NO_3$ ionic salt.

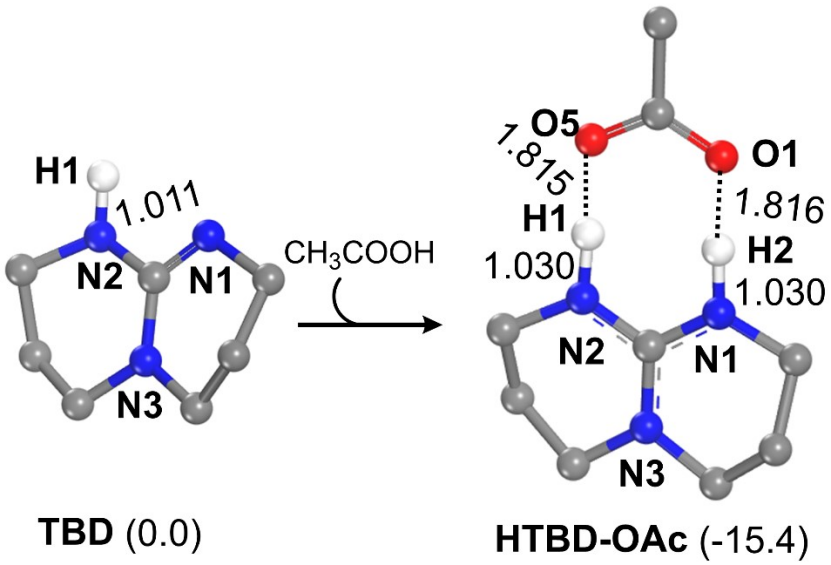


**Fig S14** The formation of HTBD-OAc. Distances are in angstrom. The Gibbs energy changes are given in parentheses (kcal/mol)**.**

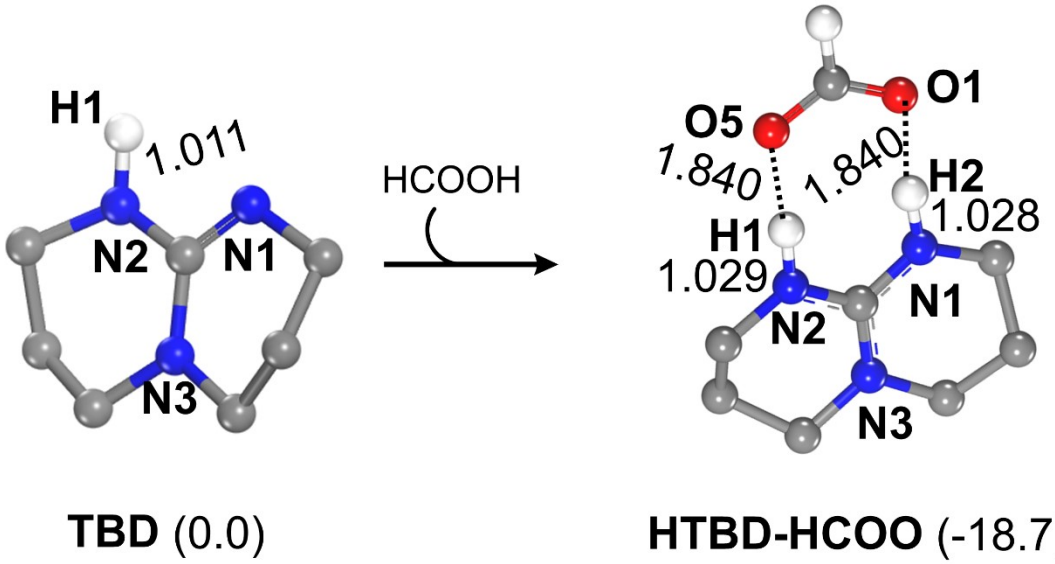


**Fig S15** The formation of HTBD-COO. Distances are in angstrom. The Gibbs energy changes are given in parentheses (kcal/mol)**.**

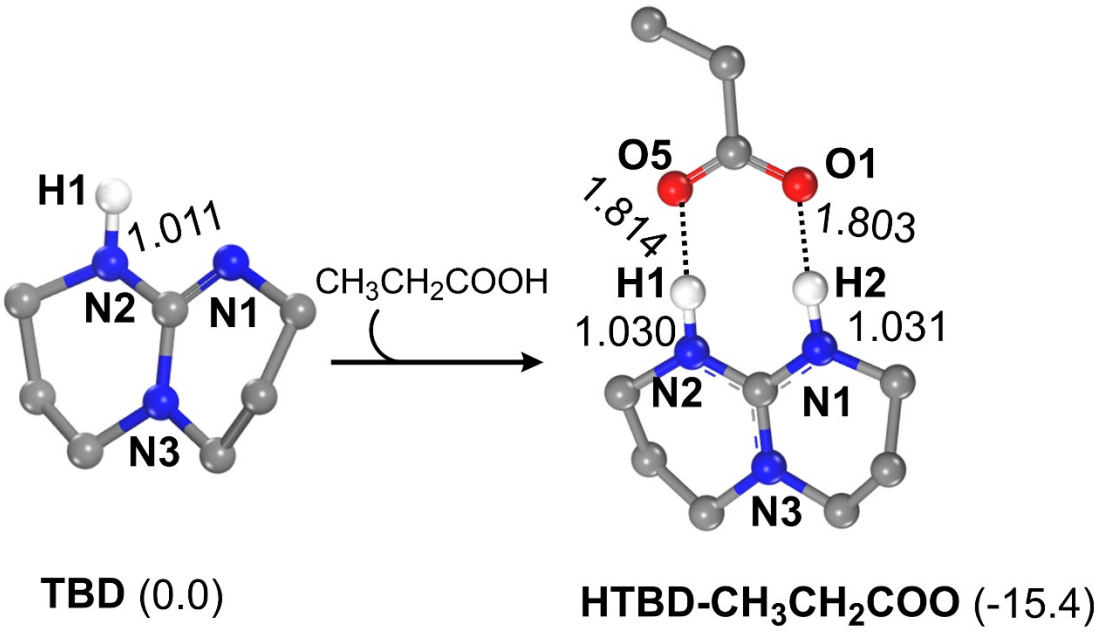


**Fig S16** The formation of HTBD-$CH_3CH_2OO$. Distances are in angstrom. The Gibbs energy changes are given in parentheses (kcal/mol)**.**

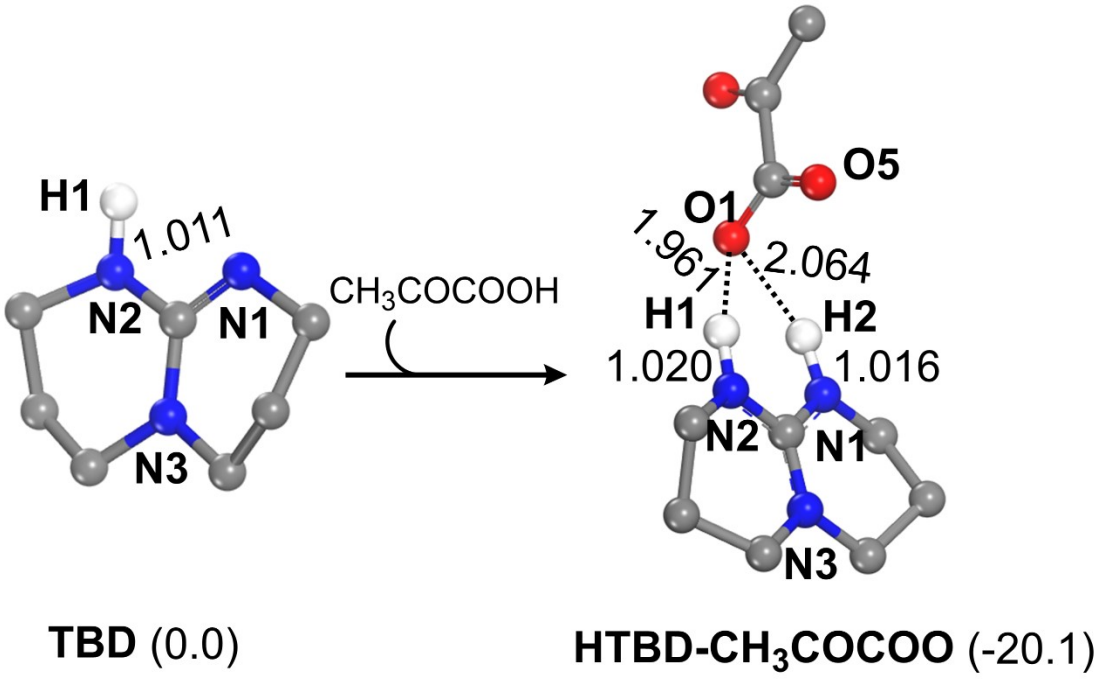


**Fig S17** The formation of HTBD-$CH_3COCOO$. Distances are in angstrom. The Gibbs energy changes are given in parentheses (kcal/mol)**.**

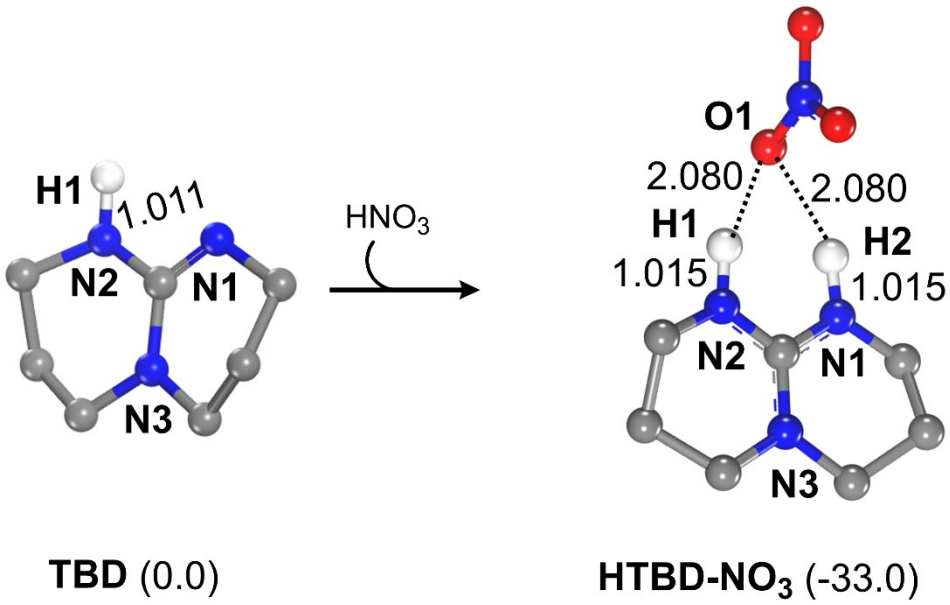


**Fig S18** The formation of HTBD-$NO_3$. Distances are in angstrom. The Gibbs energy changes are given in parentheses (kcal/mol)**.**

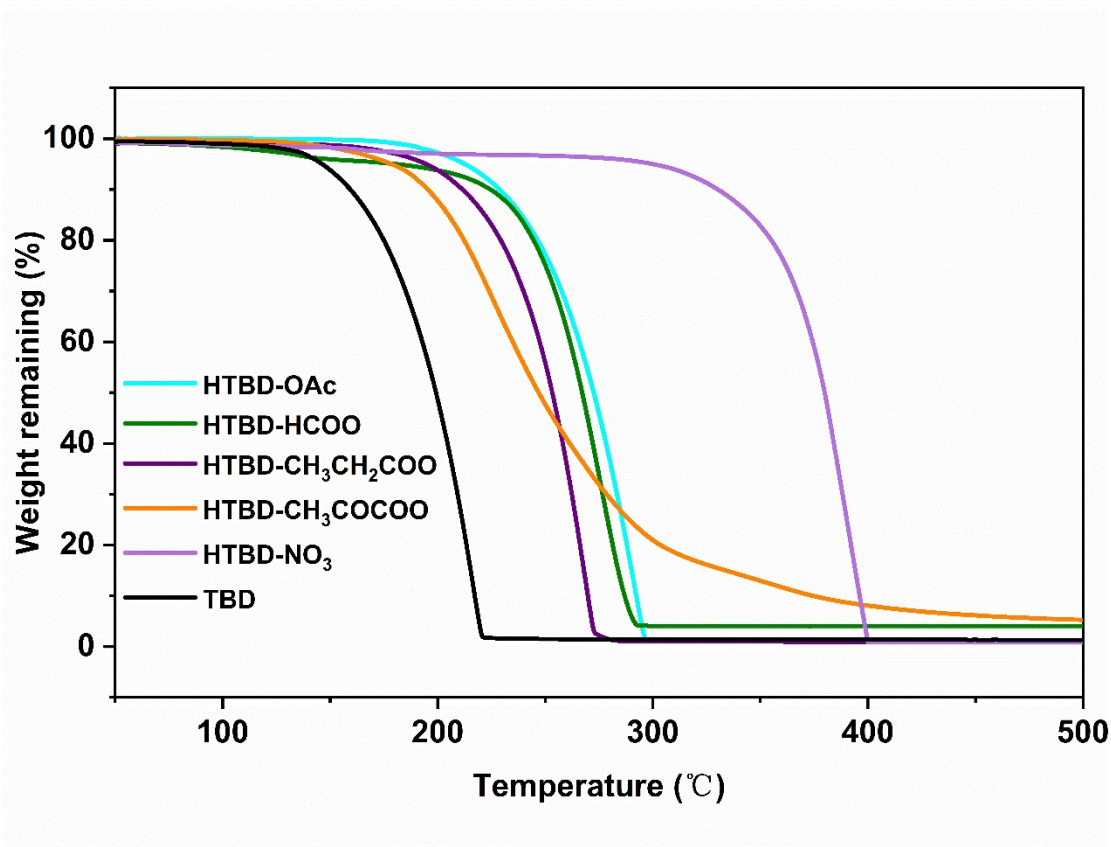


**Fig S19.** The TGA curves for TBD and TBD-based ionic salts.

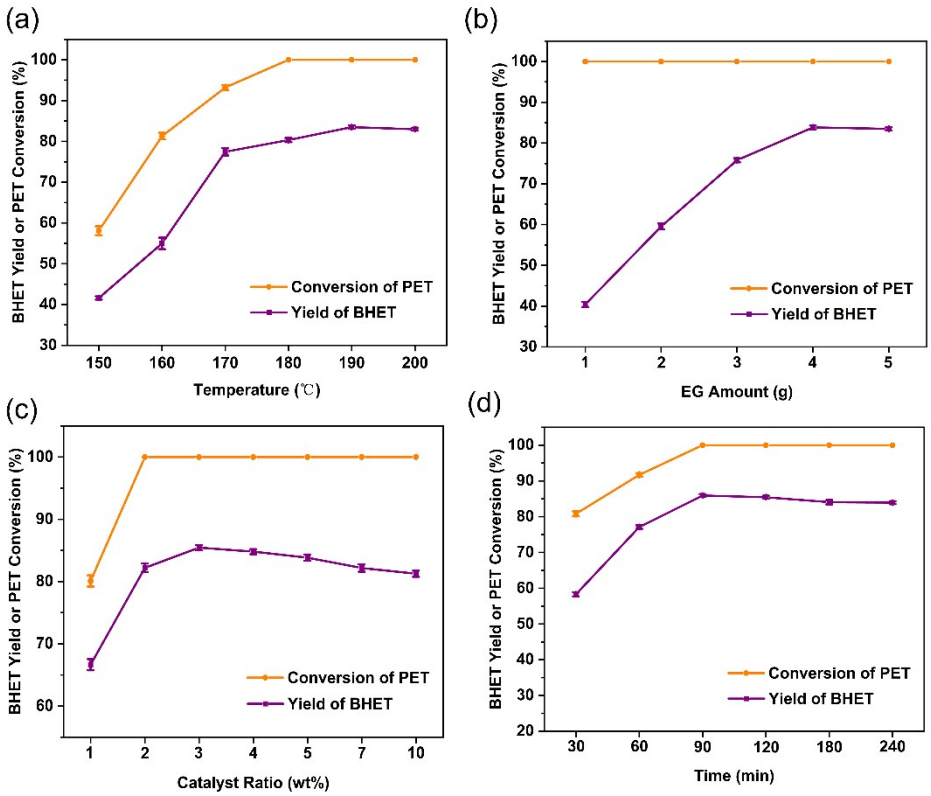


**Fig S20.** Effect of (a)reaction temperature; reaction conditions: PET 1 g, EG 5 g, catalyst 50 mg, reaction time 2 h; (b) amount of EG; reaction conditions: PET 1 g, catalyst 50 mg, reaction temperature 190°C, reaction time 2 h; (c) amount of catalyst; reaction conditions: PET 1 g, EG 4 g, reaction temperature 190°C, reaction time 2 h; and (d) reaction time; reaction conditions: PET 1 g, EG 4 g, catalyst 30 mg, reaction temperature 190°C; on PET glycolysis reaction catalyzed by HTBD-OAc.

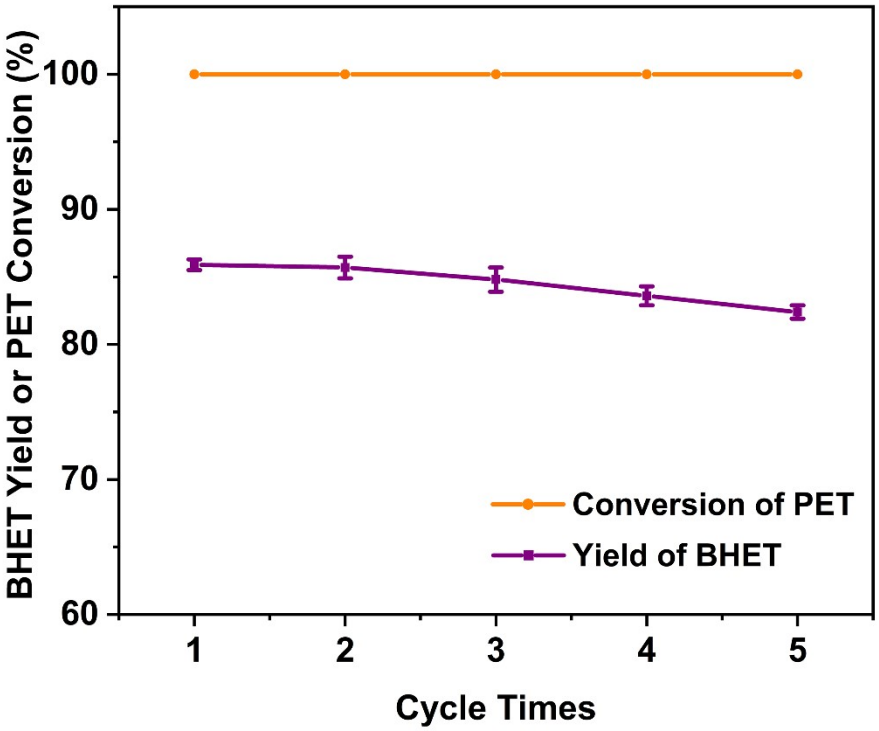


**Fig S21.** Reusability of the HTBD-OAc protic ionic salt. Reaction conditions: PET, 1.0 g; EG, 4.0 g; catalyst,50mg; atmospheric pressure at 190 °C; 90 min.

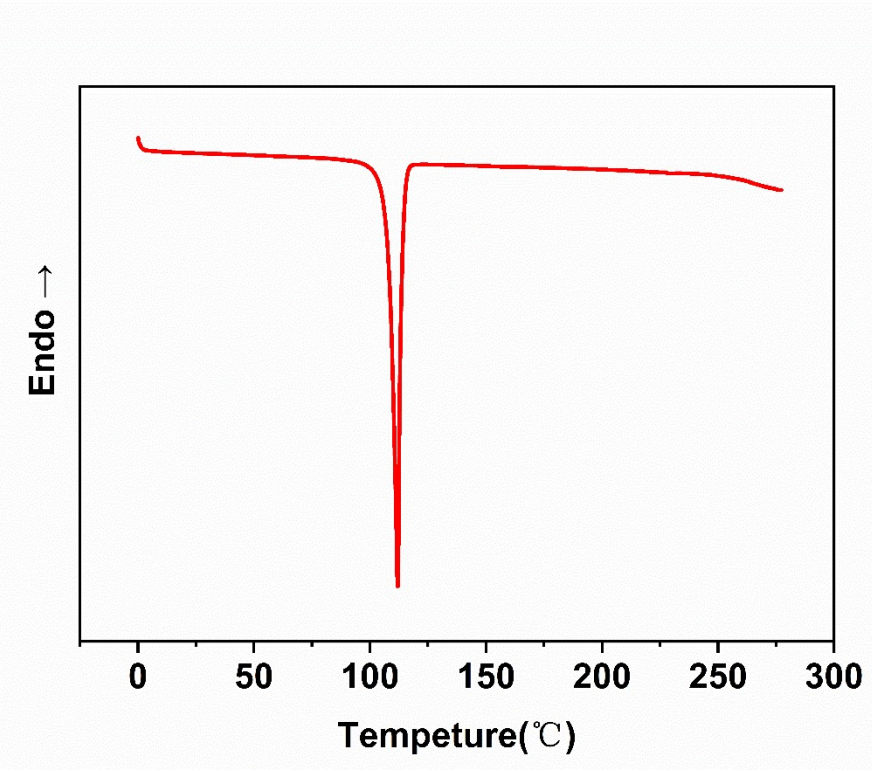


**Fig S22.** The DSC curve of the main product

1 P. Hohenberg, W. Kohn, *Phys. Rev.* **1964**, *136*, B864-B871 10.1103/PhysRev.136.B864.
2 W. Kohn, L. J. Sham, *Phys. Rev.* **1965**, *140*, A1133-A1138 10.1103/PhysRev.140.A1133.
3 J. D. Chai, M. Head-Gordon, *Phys. Chem. Chem. Phys.* **2008**, *10*, 6615-6620 10.1039/b810189b.
4 M. Mao, C. Luo, T. P. Pollard, S. Hou, T. Gao, X. Fan, C. Cui, J. Yue, Y. Tong, G. Yang, T. Deng, M. Zhang, J. Ma, L. Suo, O. Borodin, C. Wang, *Angewandte Chemie-International Edition* **2019**, *58*, 17820-17826 10.1002/anie.201910916.
5 A. V. Marenich, C. J. Cramer, D. G. Truhlar, *The Journal of Physical Chemistry B* **2009**, *113*, 6378-6396 10.1021/jp810292n.
6 R. Ditchfield, W. J. Hehre, J. A. Pople, *J. Chem. Phys.* **1971**, *54*, 724-728 10.1063/1.1674902.
7 T. Clark, J. Chandrasekhar, G. W. Spitznagel, P. v. R. Schleyer, *J Comput Chem.* **1983**, *4*, 294-301 10.1002/jcc.540040303.
8 P. C. Hariharan, J. A. Pople, *Theoret. Chim. Acta* **1973**, *28*, 213−222.
9 M. J. Frisch, J. A. Pople, J. S. Binkley, *J. Chem. Phys.* **1984**, *80*, 3265-3269 10.1063/1.447079.
10 K. Fukui, *J. Phys. Chem.* **1970**, *74*, 4161-4163 10.1021/j100717a029.
11 K. Fukui, *Acc. Chem. Res.* **1981**, *14*, 363-368 10.1021/ar00072a001.
12 M. Mammen, E. I. Shakhnovich, J. M. Deutch, G. M. Whitesides, *Journal of Organic Chemistry* **1998**, *63*, 3821-3830 10.1021/jo970944f.
13 M. J. Frisch, G. W. Trucks, H. B. Schlegel, G. E. Scuseria, M. A. Robb, J. R. Cheeseman, G. Scalmani, V. Barone, G. A. Petersson, H. Nakatsuji, X. Li, M. Caricato, A. V. Marenich, J. Bloino, B. G. Janesko, R. Gomperts, B. Mennucci, H. P. Hratchian, J. V. Ortiz, A. F. Izmaylov, J. L. Sonnenberg, D. Williams-Young, F. Ding, F. Lipparini, F. Egidi, J. Goings, B. Peng, A. Petrone, T. Henderson, D. Ranasinghe, V. G. Zakrzewski, J. Gao, N. Rega, G. Zheng, W. Liang, M. Hada, M. Ehara, K. Toyota, R. Fukuda, J. Hasegawa, M. Ishida, T. Nakajima, Y. Honda, O. Kitao, H. Nakai, T. Vreven, K. Throssell, J. A. Montgomery, Jr., J. E. Peralta, F. Ogliaro, M. J. Bearpark, J. J. Heyd, E. N. Brothers, K. N. Kudin, V. N. Staroverov, T. A. Keith, R. Kobayashi, J. Normand, K. Raghavachari, A. P. Rendell, J. C. Burant, S. S. Iyengar, J. Tomasi, M. Cossi, J. M. Millam, M. Klene, C. Adamo, R. Cammi, J. W. Ochterski, R. L. Martin, K. Morokuma, O. Farkas, J. B. Foresman, D. J. Fox, *Gaussian16, Revision A.03; Gaussian, Inc., Wallingford, CT* **2016**.
14 T. Lu, Q. Chen, *J Comput Chem* **2022**, *43*, 539-555 10.1002/jcc.26812.
15 T. Lu, F. Chen, *Journal of Computational Chemistry* **2012**, *33*, 580-592 https://doi.org/10.1002/jcc.22885.